Short Communication

Titanate matrices as potential corrosion inhibitor nanocontainers

Yongming Tang [a,*], Ziyi Cao [a], Jinqiu Xu [a], Hui Cang [b,*], Wenheng Jing [c,d]

[a] School of Science, Nanjing University of Technology, Nanjing 210009, PR China
[b] College of Chemical Engineering and Biological, Yancheng Institute of Technology, Yancheng 224051, PR China
[c] College of Materials Science and Engineering, Nanjing University of Technology, Nanjing 210009, PR China
[d] State Key Laboratory of Material-Oriented Chemical Engineering, Nanjing 210009, PR China

A B S T R A C T

Layered titanates as inhibitor nanocontainers were studied in this paper. Pyridine as a typical inhibitor was introduced into the titanate matrices and its extraction from the matrices was studied. The results show that the increase of pH of media favors the extraction of pyridine from the matrices. The layered structure of titanate containers remains stable after both introduction and extraction of pyridine. Additionally, corrosion inhibition measurements also confirm the effective release of pyridine from the titanate nanocontainers.

© 2014 Elsevier Ltd. All rights reserved.

1. Introduction

Introducing inhibitors into organic coatings is one of the most common ways to improve protection of the coatings in corrosive environmental. However, the direct introduction of corrosion inhibitors in the passive barrier coatings may have negative effect on their corrosion resistance [1]. Zheludkevich et al. reported that only if the solubility and release rate is appropriate in the corrosion region will the inhibitor work [1]. A promising strategy to overcome these problems is the encapsulation of inhibitors within nanoscale containers [2–5]. Some nanotube materials such as titanium dioxide (TiO_2) and halloysite with a hollow tubular structure were investigated as reservoirs of corrosion inhibitors [6,7]. Inhibitive molecules stored in the nanotubes can be released by the change of pH of corrosive environment or the dissolution of metal-inhibitor stopper at the tube ending [6–8]. Recently, layered nanomaterials with ion-exchange capability such as layered double hydroxides (LDHs) have been widely studied as reservoirs of corrosion inhibitors. LDHs consist of stacks of positively charged mixed metals hydroxide layers between which anionic species and solvent molecules are intercalated [9]. The release of inhibitors in LDHs can be controlled by ion-exchange with aggressive corrosive chloride ions [9–11].

Hydrogen titanates with layered structure are of distinct intercalation capability toward some organic molecules [12]. Among the titanates, $H_xTi_{2-x/4}\gamma_{x/4}O_4$ is most interested due to the lowest charge density [13]. The host layers of the matrices are of lepidocrocite-type in which TiO_6 octahedra connect to each other by edge sharing to produce a two-dimensional sheet. Some compounds containing nitrogen with lone pair electrons can be easily incorporated into the interlayer space of the titanate matrices by sharing electron with layer sheets [14,15]. The intercalation capability of layered titanates shows potential application in inhibitor reservoirs. However, there were few reports about titanate nanocontainers of inhibitors, especially in extraction of inhibitors from the interlayer space of titanates. In this paper, a well-known inhibitor, pyridine (Py), was used to study the storage and release property of $H_xTi_{2-x/4}\gamma_{x/4}O_4$ nanocontainers. The present study shows broad perspectives in utilizing the titanate nanocontainers as an alternative inorganic matrix for feasible inhibitor reservoirs.

2. Experimental

The titanate nanocontainers with the chemical formula of $H_xTi_{2-x/4}\gamma_{x/4}O_4 \cdot nH_2O$ ($x \sim 0.7$, γ: vacancy; abbreviated as HTi) were prepared by solid-state and ion-exchange reaction as previously reported [15]. To synthesize $Cs_xTi_{2-x/4}\gamma_{x/4}O_4$, mixture of Cs_2CO_3 and TiO_2 with a molar ratio of 1:5.3 was calcined at 800 °C for 1 h, and then was ground at room temperature. Afterwards, the mixture was calcined at 800 °C for 20 h twice separated by grinding. The white $Cs_xTi_{2-x/4}\gamma_{x/4}O_4$ powder (2 g) was then stirred in

100 mL of 1 M HCl solution at room temperature for 3 d to achieve the ion-exchange of Cs⁺. The HTi product was filtered, washed with ultrapure water and dried under vacuum. Introduction of Py into HTi to obtain Py–HTi complex was conducted following the procedure proposed by Sasaki [16]: 20 mL of pyridine was added to 0.2 g of HTi, and then the mixture was shaken at 25 °C for a week. Afterwards, the solids were filtered, washed with ethanol and dried under reduced vacuum.

To investigate the release performance, 0.1 g/L Py–HTi was added to buffer solutions with different pH at room temperature, and the concentration of Py released into the solutions was determined by UV spectrophotometer (UV-1200) at 250 nm at 1 min of interval. The initial storage of Py in the titanate matrices was determined by elemental analysis as mentioned in reference [12]. Accordingly, the released percentages were calculated by ratioing the amount of released Py to the initial storage. After the release tests, the residual solids were separated by filtration, washed with ethanol and dried in vacuum overnight. The nanocontainers before and after the releasing tests were identified by X-ray diffraction analysis (XRD) (Miniflex 600) using Cu Kα radiation (λ = 0.15406 nm). Infrared spectra were recorded on a FT-IR spectrophotometer (Nicolet 870) against the background spectrum of KBr. Scanning electron microscope (SEM) (S-4800) was used to observe the microstructure of nanomaterials. All chemicals, TiO_2, Cs_2CO_3, NaAc, pyridine (Py) and HAc were of reagent grade, and were used without further purification.

For electrochemical test, classical three-electrode cell was used, comprising a mild steel disk embedded in Teflon holder using epoxy resin with an exposed area of 0.785 cm^2 as the working electrode, a saturated calomel reference electrode (SCE) with a Luggin capillary and a platinum foil counter electrode. The working electrode was abraded with wet SiC paper (up to 2000 grit), cleaned with ethanol and washed with ultrapure water prior to use. 0.01 M HCl was synthesized by dilution of analytical grade of 37% HCl with ultrapure water and the content of Py–HTi complex in the corrosive media was 2 g/L. After the preset releasing periods, the titanate matrices were separated from the solutions rapidly by filtration under reduced pressure and the filtrates were used for electrochemical impedance spectroscopy (EIS) measurements. Prior to EIS tests, to ensure the steady state of the corrosion system, the working electrode was immersed in the unstirred test solutions for 30 min at room temperature until a steady open circuit potential. All of the spectra were recorded at open circuit potential (potentiostatic mode) while a 10 mV sinusoidal perturbation was applied in a frequency range from 100 kHz to 10 mHz. All of the electrochemical tests were carried out on an IVIUM Vertex electrochemical workstation controlled by IVIUM software.

3. Results and discussion

Fig. 1a and b shows the XRD patterns of nonstoichiometric cesium titanate (CsTi) and HCl-treated product HTi. It is clear that the diffraction peak (2θ = 9.58°) corresponding to (0 2 0) plane of HTi is slightly lower than that of CsTi (2θ = 10.44°). This is due to the exchange and substitution of Cs⁺ in CsTi by H_3O^+ in the solution. XRD patterns of the complex after incorporation of pyridine are given in Fig. 1c. Upon the incorporation of pyridine, the (0 2 0) peak of Py–HTi shifts to a much lower 2θ angle (7.91°), and the interlayer distance increases from 9.2 Å to 11.2 Å. This result indicates that pyridine is successfully intercalated into the interlayer space of HTi to expand the interlayer distance [16]. In order to investigate the release of pyridine from Py–HTi, the complex was stirred in a buffer solution with pH = 6. It can be seen that the (0 2 0) peak after stirred shifts to a higher 2θ angle (9.88°) similar to that of HTi (Fig. 1d). Therefore, we can infer that pyridine has been released from the titanate complex and both storage and
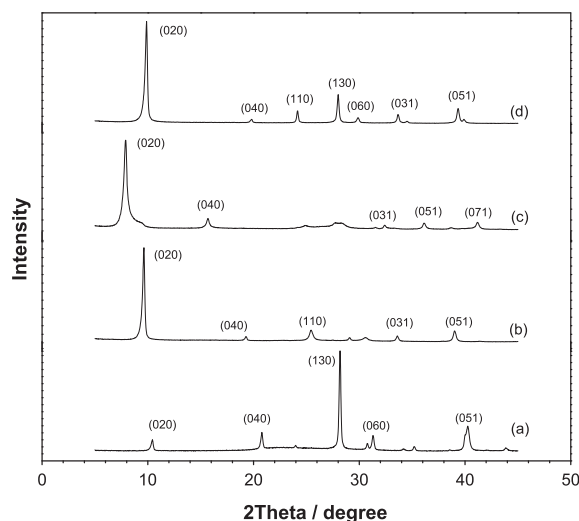

Fig. 1. X-ray diffraction patterns of (a) $Cs_xTi_{2-x/4}\gamma_{x/4}O_4$, (b) HTi, (c) Py–HTi and (d) HTi after extraction.

release of the guest molecules do not change or destroy the layered structure of host titanate containers.

FT-IR spectroscopy shows further evidence for the incorporation and release of pyridine in the titanate containers (Fig. 2a). The broad absorption band at 3420 cm^{-1} is assigned to stretching vibrations of water molecules in the layer structure [17]. The bands at 682, 754, 1251, 1487, 1539, and 1634 cm^{-1} observed in Fig. 2a(II) correspond to absorption of pyridinium ion [16,18]. Among those bands, the absorption band at 1634 cm^{-1} is attributed to the stretching vibration of pyridine ring. The relatively strong absorptions at 1539 and 1487 cm^{-1} are attributed to the skeletal vibration of pyridine ring. The peak at 1251 cm^{-1} is in-plane bend of N—H bond, indicating the combination between pyridine and the layers of HTi. Two weak bands appear at 754 and 682 cm^{-1}, which are caused by the out-of-plane bending vibrations of C—H bond on pyridine ring. In addition, the bands at 3000–3100 cm^{-1} are the symbol of aromatic C—H stretching vibrations [17]. From the above results, it is concluded that pyridine has been incorporated into the interlayer space of HTi. Fig. 2a(III) shows the FTIR spectra of the sample after stirred in pH = 6 buffer solution and washed with ethanol. It is clear that those absorption bands corresponding to pyridinium ion disappear, which means the extraction of pyridine from the interlayer space of the titanate complex. Moreover, the spectra of the sample after release of pyridine is almost identical to that before the intercalation of pyridine, and the broad absorption band between 400 and 1000 cm^{-1} corresponding to Ti—O and Ti=O vibrations remains unchanged at all times [19]. This indicates that the framework of the titanate matrices is not affected during the incorporation and extraction of pyridine. This result is consistent with that of XRD measurements.

SEM images of the titanate matrices before and after the removal of pyridine are presented in Fig. 2b. The pristine HTi displays granular morphology with a primary particle size of 200–400 nm. After the incorporation and extraction of pyridine, the morphology remains almost unchanged, which can be regarded as an additional evidence for the maintenance of the titanate framework during the storage and release of inhibitors.

The extraction behavior of pyridine stored in the titanate containers was investigated by testing the dependence of the concentration of pyridine released into the solution on reaction time. Weakly acidic media were used to investigate the effect of pH on the releasing performance of pyridine at room temperature. Two stages can be seen from the releasing curves (Fig. 3a): fast releasing